UNLIMITED

TR 89014

ROYAL AEROSPACE ESTABLISHMENT

Technical Report 89014

March 1989

ENVIRONMENTAL CONSTRAINTS FOR POLAR PLATFORM DESIGN

by

A. J. Sims
P. R. Truscott
G. L. Wrenn
C. S. Dyer

Procurement Executive, Ministry of Defence
Farnborough, Hants

UNLIMITED

CONDITIONS OF RELEASE

0052184 BR-111598

********** U

********** Y

Reports quoted are not necessarily available to members of the public or to commercial organisations.

UNLIMITED

ROYAL AEROSPACE ESTABLISHMENT

Technical Report 89014

Received for printing 23 March 1989

ENVIRONMENTAL CONSTRAINTS FOR POLAR PLATFORM DESIGN

by

A. J. Sims

P. R. Truscott

G. L. Wrenn

C. S. Dyer

SUMMARY

The considerable investment implicit in large space platforms makes assessment of both their environment and their environmental interactions of utmost importance. In this Report the new factors of relevance to the Polar Platform are reviewed, and environment models and radiation transport codes are employed to assess primary and secondary particle fluxes, dose rates and energy-loss spectra. Monitors are described which can improve the data base.

Departmental Reference: Space 674

**A shortened version of this paper was presented at the 38th Congress of the International Astronautical Federation, held in Brighton, England in October 1987.*

UNLIMITED

LIST OF CONTENTS

1 INTRODUCTION

The next era in space utilisation will encompass a new generation of large spacecraft in low earth orbit (LEO) at high inclination. These Polar Platforms will provide facilities for numerous experiments and applications requiring global coverage or access to the important high latitude regions, at low or moderate altitudes. Such platforms might require manual assembly in orbit, could be manned for extended periods, or they could be serviced at intervals during their lifetime (man-tended). During the late 1960s and 70s a large number of relatively small LEO satellites were successfully flown in near polar orbits; it is now pertinent to consider the new factors which could detrimentally influence the interaction of future spacecraft with their environment so that proper account of these effects may be taken in any mission design phase.

Such new factors include marked increases in spacecraft dimensions, large quantities of potentially sensitive solid-state components, higher rates of data transfer, increased data storage capacity and longer planned lifetimes. These must be considered in the context of non-spinning, three-axis stabilisation and possible astronaut involvement. The increase in payload complexity necessarily increases the risk of mutual interference or contamination and creates considerable problems in relation to pre-launch testing, not least the expense and availability of large test facilities.

This Report addresses two main areas of concern, namely spacecraft/plasma interactions and higher energy (penetrating) radiation effects. Results of work in these areas is presented in order to demonstrate the importance to system design.

Polar Platforms are proposed as part of the NASA-ESA COLUMBUS space station mission and it is convenient to use an early specification of the ESA POLAR PLATFORM as a model for future configurations. The characteristics of the spacecraft are then as follows:

body size	: approx 10 m
deployed solar arrays	: approx 35 m
orbit	: 850 km circular, sun synchronous, 0930 descending node
period	: 102 minutes
power	: 5 kW
mass	: 5000 kg

eclipse period : 33 minutes

data rate : 500 Mb/s.

2 PLASMA INTERACTIONS

Discharges, following a charging of spacecraft by plasma sheet electrons, have caused a host of anomalies and failures in geosynchronous orbit[1]. The culpable electrons do reach ionospheric heights at high latitude and thus there is at least a potential problem of discharge damage in any high inclination orbit.

The Debye length, λ_D , gives the approximate screening distance or sheath thickness which forms around a charged body in a plasma[1];

$$\lambda_D = \left(\varepsilon_0 KT_e/n_e e^2\right)^{\frac{1}{2}} \approx 69\left(T_e/n_e\right)^{\frac{1}{2}}(m) \qquad (1)$$

where T_e = electron temperature (in °K)

n_e = electron density (in m^{-3})

ε_0 = permittivity of free space (8.854×10^{-12} Fm^{-1})

K = Boltzmann constant (1.38×10^{23} JK^{-1})

e = electronic charge (1.602×10^{-19}C).

Note that it is the electron temperature rather than the ion temperature which controls the sheath thickness, since thermal motion of the ions is negligible compared to that of the electrons. The ratio of the typical dimension of the spacecraft to the thickness of the Debye sheath is the critical factor which determines whether a spacecraft will charge to a dangerously large potential. Sheath formation neutralises the effect of isolated charge, but this effect is limited if the spacecraft is much larger than the Debye sheath. In LEO, n_e (10^{10} - 10^{12} m^{-3}) and Te (1000-5000 K)[2] vary with altitude, latitude and local time giving Debye lengths of order 5-50 mm. This is small compared to the characteristic dimension (R_0) of a satellite and the move to space platforms sees R_0 increase from typically 0.5 m to 5 m or even 50 m thereby accentuating the difference. Of course, the relevance of any analysis based upon R_0 , with the assumption of a roughly spherical satellite, has to be examined in the light of current platform designs.

Charging currents are proportional to surface area but the processes listed below can cause local charge concentrations and electric fields (differential charging) on the spacecraft surface.

(a) Energetic particles, especially electrons from the plasma sheet region, in propagating along magnetic field lines may impinge on one side of the spacecraft only and are sufficiently energetic to penetrate the potential barrier around the spacecraft.

(b) Typical ion thermal velocity at this altitude is about 1 km/s compared to the spacecraft orbital velocity of about 7 km/s. Hence the ion current to the 'front' of the spacecraft (the ram ion current) is enhanced whilst the extensive wake region behind the spacecraft is depleted of ions.

(c) Photo-emission of electrons prevents illuminated spacecraft surfaces from charging, hence a three-axis stabilised spacecraft, with some faces permanently in shadow is susceptible to differential charging.

(d) The electric $(\underline{v} \times \underline{B})$ field induced along the E-W axis of a polar orbiter due to the component of its velocity, $\underline{v}$ perpendicular to the magnetic field $\underline{B}$ reaches a maximum of about 0.4 V/m at high latitudes and could produce a significant potential difference across a large space vehicle.

(e) Differences in the secondary emission characteristics of surface materials results in adjacent surfaces reaching different equilibrium potentials given the same plasma environment.

Fig 1 is a schematic diagram which illustrates these effects. It emphasises that a combination of factors, such as energetic auroral electrons impinging on a shadowed surface at the 'rear' of the spacecraft can combine to cause some surfaces to charge. Fig 1 also shows that the simulation of such charging events is a fully three-dimensional problem, and in this case would require self-consistent solutions of the Poisson and Vlasov plasma equations in order to model the particle behaviour in the space charge sheath region.

'Floating potential' results from a balance of current components which are listed below (for a surface potential of V = 0 volts)[3]:

(a) isotropic thermal electrons
≤ 10 mA/m^2

(b) rammed thermal ions
≤ 1 mA/m^2

(c) non-rammed thermal ions
≤ 50 μA/m^2

(d) photo-emission
$\approx 20\ \mu A/m^2$.

Energetic (5-10 keV) electrons, intercepting the spacecraft in the auroral zones, could contribute a current of 200 $\mu A/m^2$ but this would be limited to a narrow band of latitude and local time. The maximum current due to trapped radiation is 1 $\mu A/m^2$.

The rate of charging $dV/dt = I/C$. Since $I \alpha R_0^2$ whilst the capacitance $C \alpha R_0$, then dV/dt is proportional to R_0 ; the larger the spacecraft, the faster it will charge. Taking $I = 200 \mu A/m^2$ and $R_0 = 10$ m gives $dV/dt = 200$ kV/s . Although the satellite passes through the auroral charging region in a fraction of a second, surfaces could charge to kilovolt potentials with consequent risk of discharge if the neutralizing ion currents are sufficiently limited. The extent of any potential problem is strongly influenced by the spacecraft geometry and the sensitivity of elements subjected to shadow and wake. Three-axis stabilisation certainly increases the probability of differential charging and the likely degradation of surfaces after long periods in space will lower discharge thresholds.

Yeh and Gussenhoven[4] have studied a number of charging events on the DMSP spacecraft, whilst Katz *et al*[5,6] have modelled the Shuttle Orbiter in similar circumstances. There is no doubt that the detailed design of Polar Platforms will raise many questions on overcoming the plasma interaction effects. A programme for the development of diagnostic techniques, involving flight hardware and computer simulation is being pursued so that these questions may be resolved.

3 PENETRATING RADIATION

3.1 Geomagnetically trapped radiation

The Polar Platform will be subjected to fluxes of high energy protons and electrons which are trapped in the geomagnetic field. Whilst operating in a polar orbit, the platform will regularly traverse two regions of high particle flux[7]; the South Atlantic Anomaly region of the inner Van Allen belt, and the 'horns' of the electron belt.

The South Atlantic Anomaly is a region of intense proton and electron fluxes extending from South America to Southern Africa at altitudes above 200 km. The Earth's magnetic field resembles that of a dipole which is slightly displaced from the centre of the Earth and is tilted with respect to the Earth's spin axis. Hence a given particle will 'mirror' at a lower altitude in one region (the South Atlantic Anomaly) than elsewhere above the Earth's surface.

The proposed sun-synchronous, 850 km, 98.8° inclination orbit means that the Polar Platform completes 14 orbits per day with a retrograde longitude shift of 25.5° per orbit. Hence, about ten orbits per day traverse a part of the SAA region; the intensity of each pass depends on the local time. Fig 2 shows a single orbit of the Polar Platform which traverses the North and South horns of the electron belts and the South Atlantic Anomaly region. The contours map equal integral fluxes for electrons with kinetic energy greater than 0.5 MeV. Fig 2 clearly shows the longitudinal extent of the Anomaly.

The flux of electrons (of kinetic energy greater than 0.5 MeV) encountered in the Anomaly approaches 10^6 particles $cm^{-2}s^{-1}$ but the Polar Platform also traverses the 'horns' of the electron belts four times every orbit. The fluxes encountered there are an order of magnitude lower than those found in the heart of the SAA at 850 km altitude and are typically 10^4 to 10^5 electrons (of energy greater than 0.5 MeV) $cm^{-2}s^{-1}$. Fig 3 shows the variation of electron flux around one Polar Platform orbit (the same one as shown in Fig 2) with horn traversals lasting between 5 and 6 minutes compared to a central SAA crossing of about 25 minutes.

During the ten daily passes through the Anomaly, the Polar Platform is subjected to fluxes of protons (of energy greater than 0.1 MeV) of between 10^2 and 10^4 particles $cm^{-2}s^{-1}$. A typical diurnal variation of proton flux, calculated with the SOFIP code (Stassinopoulos *et al*[8], 1979) is shown in Fig 4; a sequence of northbound SAA crossings is followed by sequence of southbound SAA crossings some hours later.

Accumulation of the trapped radiation fluxes over 1 day (14 orbits) leads to the integral fluence spectra of Fig 5. Although the electron fluence is two orders of magnitude higher, it is confined to energies below 10 MeV. The higher energy protons are more penetrating and contribute most to the dose received by components within the Polar Platform. In addition, the nuclear reactions of these particles can lead to single event upsets in microprocessors and memories. The mean daily fluence of protons with energies greater than 15 MeV is in excess of 10^7 cm^{-2}.

The models used to evaluate the flux levels are IGRF 1975[9] for the geomagnetic field, together with AP8MAX[10] and AE8MAX[11], which give the instantaneous proton and electron fluxes respectively for a given point in (B, L) space for solar maximum. The solar maximum models were used since solar activity will be high during much of the operational lifetime of the Polar Platform. There is

some controversy[12] concerning the method for updating these models to present day predictions, because the Earth's magnetic dipole moment is slowly decaying. If the magnetic field model is extrapolated to a future epoch (e.g. the 1990s) and then used directly with AP8MAX or AE8MAX a considerable overestimate of the flux levels is obtained. For a given altitude, the decreased value of the magnetic field would correspond to a region of higher flux in the models, which have been calculated for an epoch some 25 years earlier. This study used the method recommended by NASA which involved extrapolating the field model back to 1970 when the particle models were developed; the results applicable to solar maximum were then used directly. Uncertainties of at least a factor of two still apply and further measurements are required to adequately characterise this régime. In addition the particle fluxes are highly anisotropic and this should be modelled more thoroughly to allow for spatial variations within a three-axis stabilised platform.

3.2 Cosmic rays and solar protons

Outside the Earth's magnetosphere there are two major sources of penetrating particles, a continuous flux of cosmic rays comprising protons and heavier ions together with bursts of protons and ions originating from solar flares. The Earth's geomagnetic field offers some natural protection against such particles because of Lorentz deflection. A cosmic ray particle approaching the Earth near the geomagnetic equator must cross a large number of magnetic field lines to reach LEO altitudes and will be deflected unless it has a very high energy; at higher latitudes there is less protection. Since the Polar Platform regularly crosses the geomagnetic pole regions, it will then be subjected to large fluxes of extra-magnetospheric particles.

The attenuation of the cosmic ray flux by the geomagnetic field is based on the model of Adams[13]. This method calculates the cut-off rigidity (momentum/unit charge) that a particle must possess to reach a given point in the magnetic field. A 'transmittance' function is produced by averaging the cut-offs over a 2-day section of the Polar Platform orbit.

Solar flares occur, on average for about 2% of the time and the resulting proton spectrum is highly variable in both energy and intensity. Fig 6 shows how the low energy protons from a typical flare completely dominate the mean differential proton spectrum seen by the Polar Platform shortly after the event. In addition, there will be many protons of energy less than 10 MeV but these are easily shielded. The flux of cosmic rays is very low (less than 4×10^{-5} $cm^{-2}s^{-1}$ MeV^{-1}) but it does contain particles which are both energetic and highly ionising.

Infrequently, an Anolamously Large Event (ALE) will occur when very large fluxes of solar protons with energies up to several hundred MeV are produced. Such events are rare (one or two per solar cycle) but the dose from a single ALE could exceed the dose accumulated during the rest of a Polar Platform mission.

3.3 Effects of shielding and estimates of energy deposition

The effects of shielding of sensitive equipment from the penetrating radiation described in sections 3.1 and 3.2 have been assessed by three methods:

(a) Application of the program SHIELDOSE[14], which makes use of pre-calculated depth versus dose data for various shielding materials.

(b) Using Monte Carlo particle transport codes (HETC[15] and MORSE[16]) to model in detail the physics of the interactions of high energy protons in irradiated materials, including the transport of all secondary, tertiary, etc particles produced through nuclear interactions.

(c) Using the program LET[13] which calculates the integral and differential Linear Energy Transfer (LET) spectra experienced behind various shielding materials for a given cosmic ray spectrum.

The first two methods were used to predict the average dose rate which would be experienced by a silicon detector at various depths within a slab. Fig 7 shows the contributions made to the total dose received during 1 day from the trapped protons, electrons and bremsstrahlung, as calculated by SHIELDOSE. This indicates that at very low levels of shielding the energy deposition rate is dominated by electrons, most of which are stopped in the first few millimetres of material. At depths greater than approximately 3 mm (0.8 g/cm^2) the dose from the trapped protons begins to dominate.

The results from Monte-Carlo simulations of trapped proton transport are given in Figs 8 and 9. Shielding thicknesses of up to 200 g/cm^2 have been considered. The dose rates predicted by these simulations (Fig 8) are on average 30% higher than the SHIELDOSE results. This is, however, expected since the proton source used in the particle transport simulations was considered to be unidirectional and impinging on the slab normal to its surface in order to represent a worst case situation, whereas the source used to obtain the SHIELDOSE results was assumed to be omnidirectional.

Fig 9 shows the average neutron fluence expected per day, again as a function of shielding thickness. It can be seen that this rises with increasing shield thickness, reaching a maximum at approximately 30 g/cm^2 (111 mm) of

aluminium when the daily neutron fluence is 4×10^6 per cm^2 for neutrons with energy <15 MeV and 2×10^5 per cm^2 for those with energy >15 MeV. This build-up of secondary neutrons can lead to enhanced upset rates in devices and to increased noise rates in certain sensors.

From Fig 9 one also notices a hardening of the neutron spectrum with depth. This is because neutrons with higher energies (several 10s to 100s of MeV) are produced by an intra-nuclear cascade[17] in which the neutrons are 'torn' out of the nucleus by an incoming energetic particle (usually a primary inner belt proton). The momentum of these cascade neutrons approximately follows the same direction as the primary particle, and so they propagate deeper into the shield. The low energy neutrons, however, are usually produced by evaporation from the spalled nucleus a relatively long time afterwards ($>10^{-14}$ seconds). Since the nucleus can be considered to be stationary the evaporation neutrons are emitted isotropically.

A further consequence of such nuclear cascades is the radioactivity induced in spaceborne materials. Whilst dose rates from this contribution are low compared with the prompt cascades, significant background rates are produced in sensitive scientific instruments. In addition the levels of radioactivity induced at high altitude might well provide a significant biological dose contribution if the platform is returned to lower altitudes for servicing by astronauts. Calculations of radioactivity induced in scientific instruments have been performed[18] and can be extended to assess handling problems.

One advantage of using SHIELDOSE is that the resultant dose versus depth results can be easily corrected for a particular geometry, and in Fig 10 the dose rate on the inner surface of a spherical shell is plotted as a function of shell thickness, again for the average Polar Platform radiation environment. It is instructive to compare these results with recent experimental data obtained from the Defence Meteorological Satellite Program[19] (DMSP) F7 satellite, launched in November 1983. Its orbit is almost identical to that proposed for the Polar Platform, *ie* 840 km, sun synchronous. This spacecraft carried dosimeters mounted beneath four hemispherical aluminium domes of various thicknesses. The DMSP F7 results are given in Table 1, together with the SHIELDOSE predictions for dose rates behind the appropriate thickness of shell. Agreement between the average measured dose rate and the SHIELDOSE results is better than 11%.

Table 1

Comparison of DMSP data with SHIELDOSE results

SAA proton doses in rads(Si)/day					
Shielding thickness (g/cm^2):		0.55	1.55	3.05	5.91
DMSP data:	09.11.84	1.20	0.83	0.63	0.48
	26.11.84	1.22	0.77	0.57	0.44
	03.02.85	1.18	0.80	0.59	0.46
SHIELDOSE predictions:		1.27	0.83	0.61	0.41

In Fig 11 the integral cosmic ray particle flux which will be experienced beneath 6.35 mm (0.25 inch) of aluminium is plotted as a function of the particle's linear energy transfer using results calculated by the program LET. Linear energy transfer is a measure of the ionisation power of a particle and is defined as the amount of energy deposited by the particle per unit path length (in units of density × thickness) through a specified material (in this case silicon). Upset thresholds for microelectronics are conveniently expressed in terms of LET with the integral fluxes above threshold readily related to upset rates.

The solid curve in Fig 11 refers only to galactic cosmic rays, the step-like nature of the spectrum results from the different nuclei making up the source radiation. Because of the minimum ionizing nature of relativistic particles each element deposits only a narrow range of energies (LET). The first drop in the spectrum corresponds to a fall in the intensity of cosmic ray protons which mostly deposit energy at a rate less than 2 MeV cm^2g^{-1} behind the aluminium shield, whilst the second step at approximately 8 MeV cm^2g^{-1} corresponds to a similar fall in intensity in helium.

The dashed curve in Fig 11 shows the LET spectrum expected from both galactic and solar cosmic rays during a mean solar flare. Fluxes of protons and alpha particles are greatly increased in the range 10-200 MeV because of the low amount of geomagnetic shielding over the poles. Protons and alphas with energy >35 MeV/nucleon are able to penetrate 6.35 mm of aluminium shielding. Consequently the LET spectrum is greatly enhanced at the lower LET end (1.5-100 MeV cm^2g^{-1}).

4 DISCUSSION

Results have been presented on the energetic primary and secondary radiation environment to be expected for the Polar Platform based upon some of the best available environmental models and radiation transport codes.

However, it must be realised that all the models have their limitations and that their correct application is still a matter of some debate. For instance the prediction of trapped proton fluence arising from the South Atlantic Anomaly is of great importance for space platforms but is still uncertain due to the evolving nature of the Earth's magnetic field. There is thus an ongoing need to monitor the relevant environments, both in order to improve the models and to interpret the functioning of equipment, warn of failures and to correct data. To this end a "Cosmic Radiation Effects and Activation Monitor" (CREAM) and a "Shuttle Activation Monitor" (SAM) have been designed for deployment as Shuttle mid-deck experiments.

The CREAM experiment employs a 10 cm^2 array of pin diodes with pulse-height analysis to give the LET spectra as a function of time, geomagnetic location and spacecraft shielding. This is complemented by packages of passive detectors comprising plastic track detectors for the detection of heavy ions, activation foils for the detection of neutrons and thermoluminescent dosimeters for the monitoring of total dose. Using astronaut deployment, a number of mid-deck locations affording various amounts of shielding can be monitored. The SAM experiment is a collaborative venture involving the University of Florida, NASA Goddard Space Flight Center and Space Department, RAE. In this experiment active scintillation detectors are employed to monitor the secondary gamma rays emitted by the Shuttle, together with the radioactivity induced in spacecraft and detector materials. The CREAM experiment was initially scheduled for deployment by the UK astronaut on STS-61H which was cancelled in the wake of the Challenger tragedy. It is now hoped that SAM and CREAM may share flights early in the new Shuttle programme as the complementary nature of the radiations monitored would maximise the utility of the data. The CREAM package is readily adaptable to serve as a monitor for free-flying spacecraft and platforms and flight opportunities are being sought to cover a variety of orbits including the Polar Platform.

5 CONCLUSIONS

It has been shown that the size increase of future Polar Platforms compared with current spacecraft warrants further investigation and modelling of the deleterious influences of charging and plasma wake phenomena.

State-of-the-art radiation belt and shielding models have been used to assess dose rates to electronics. Uncertainties of a factor of two still exist and the influence of particle anisotropies requires further modelling. While the total dose is relatively benign at these altitudes (less than 1000 km), the increase in desired mission lifetime requires that adequate attention still be paid to device hardening.

Of probably greater significance is the exposure to cosmic ray and solar flare heavy ions in the polar region and the frequent passages through intense proton fluxes in the South Atlantic Anomaly. These aspects of the environment can lead to very significant upset rates in certain memories and processors as well as to enhanced noise levels in sensor elements. There are still considerable uncertainties with respect to particle fluxes, composition and the influence of anisotropies and shielding. In addition, there are very few measurements on proton-induced upset cross-sections.

There is clearly a need for further modelling of the environment and its effects in conjunction with environment measurements and both in-orbit and ground-based characterisation of key technologies.

REFERENCES

No.	Author	Title, etc
1	E.C. Whipple	Potentials of surfaces in space. *Rep. Prog. Phys.*, 44, 1197 (1981)
2	J.K. Hargreaves	The upper atmosphere and solar terrestrial relations. Van Nostrand Reinhold Co. Ltd. (1979)
3	I. Katz *et al*	A three dimensional dynamic study of electrostatic charging in materials. NASA CR-135256 (1977)
4	H.C. Yeh M.S. Gussenhoven	The statistical electron environment for DMSP eclipse charging. *J. Geophys. Res.*, 92, 7705-7715 (1987)
5	I. Katz D.E. Parks	Space shuttle orbiter charging. *J. Spacecraft and Rockets*, 20, 22-25 (1983)
6	D.L. Cooke *et al*	A three-dimensional calculation of shuttle charging in polar orbit. NASA CR 2359, 205-228 (1985)
7	E.G. Stassinopoulos	World maps of constant B, L and flux contours. NASA SP-3054 (1970)
8	E.G. Stassinopoulos *et al*	SOFIP - a short orbital flux integration program. NASA NSSDC/WDC-A-R&S 79-01 (1979)
9	IAGA Division 1 Study Group	International geomagnetic reference field 1975. *J. Geophys. Res.*, 81, 28, 5163-5164 (1976)
10	D.M. Sawyer J.I. Vette	AP8 trapped proton environment for solar maximum and solar minimum. NASA NSSDC/WDC-A-R&S 76-06 (1976)
11	NSSDC/WDC-A-R&S	Pre-publication data set.
12	P.D. McCormack	Radiation dose and shielding for space station. IAF/IAA-86-380 (1986)
13	J.H. Adams C.H. Tsao R. Silberberg	Cosmic ray effects on microelectronics Part 1: the near-earth particle environment. NRL Memo Report 4506 (1981)

REFERENCES (concluded)

No.	Author	Title, etc
14	S.M. Seltzer	SHIELDOSE - a computer code for space shielding radiation dose calculations. NBS Technical Note 1116 (1980)
15	T.W. Armstrong K.C. Chandler	Operating instructions for the high energy nucleon-meson transport code, HETC. ORNL-4744 (1972)
16	M.B. Emmett	The MORSE Monte-Carlo radiation transport code system. ORNL-4792-UC32 (1975)
17	T.W. Armstrong	The intra-nuclear cascade evaporation model. Computer techniques in radiation and dosimetry. Ettore Majorana International Science Series, Vol 3, pp 311-321
18	C.S. Dyer N.D.A. Hammond	Neutron capture induced radioactive background in large volume, spaceborne, NaI gamma ray spectrometers. IEEE Trans. on Nuclear Science, NS-32, 4421 (1985)
19	M.S. Gussenhoven *et al*	Ne low-altitude dose measurements. IEEE Trans. Nucl. Sci., NS-34, 3 (1987)

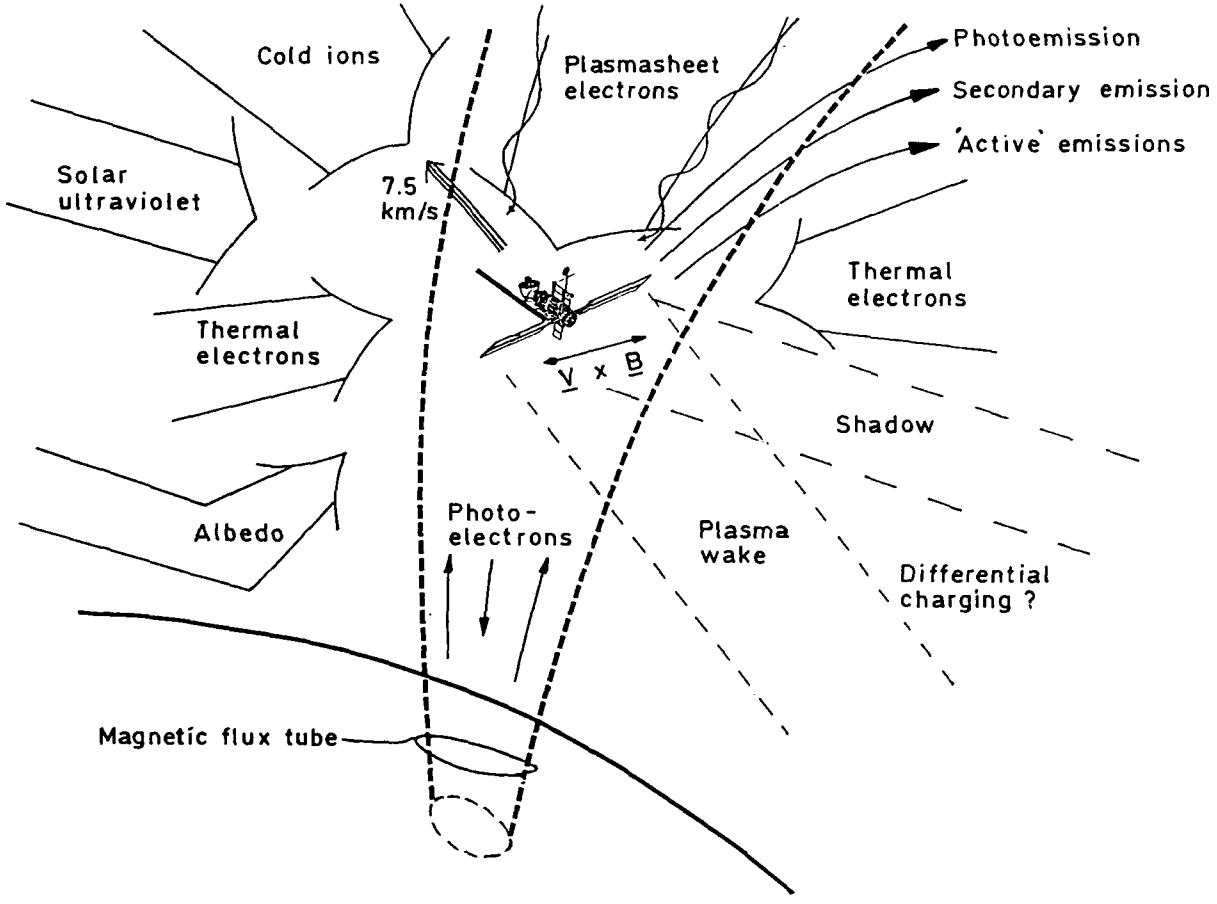

Fig 1 Plasma interactions - polar platform

Fig 1

Fig 2

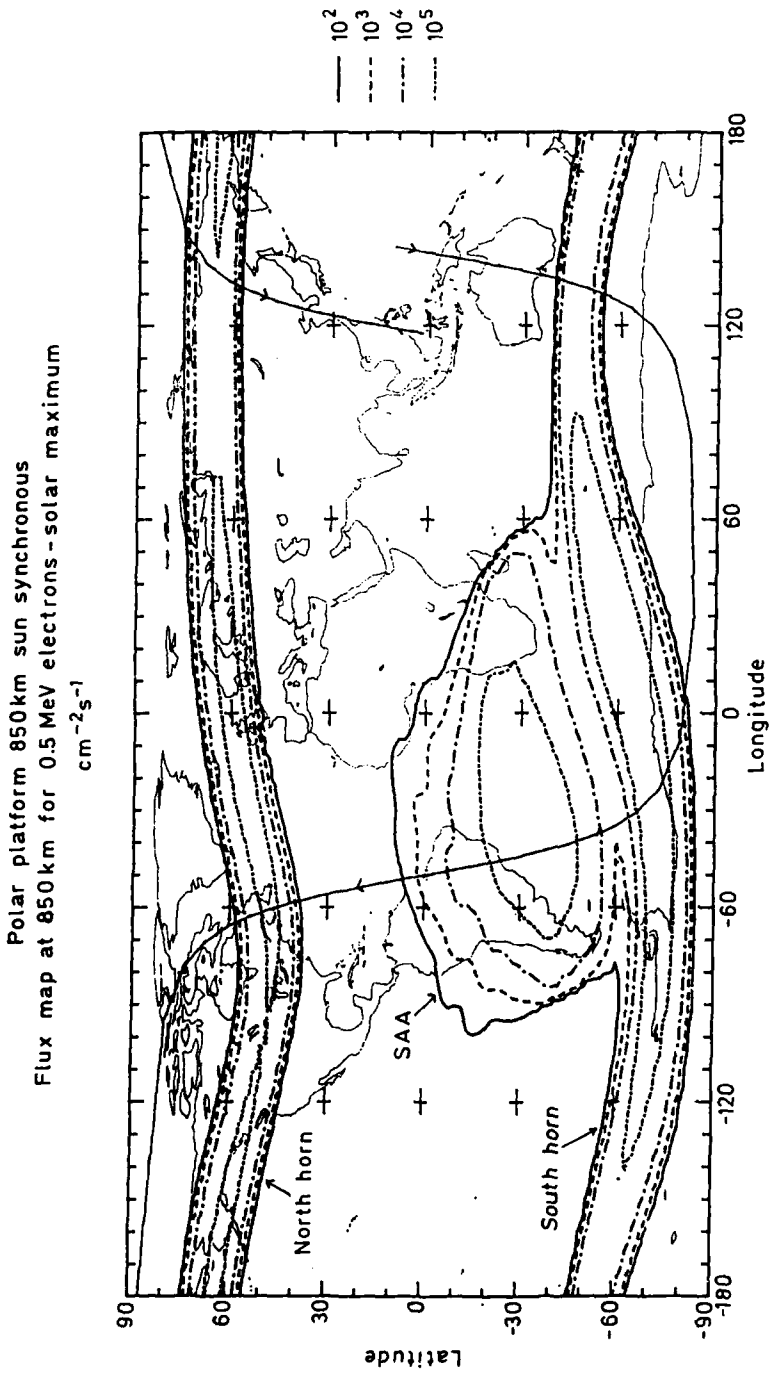

Fig 2 Electron flux contours

TR 89014

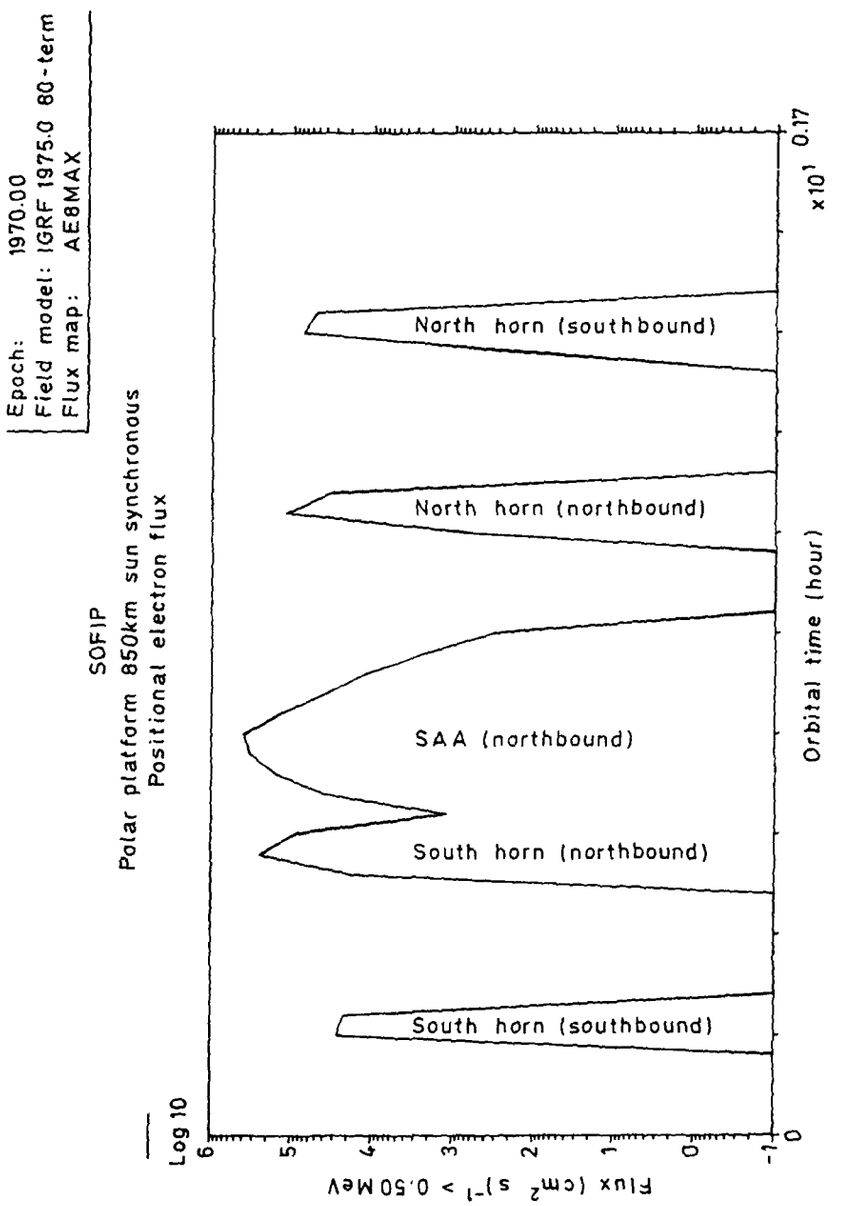

Fig 3 Positional electron flux

Fig 4

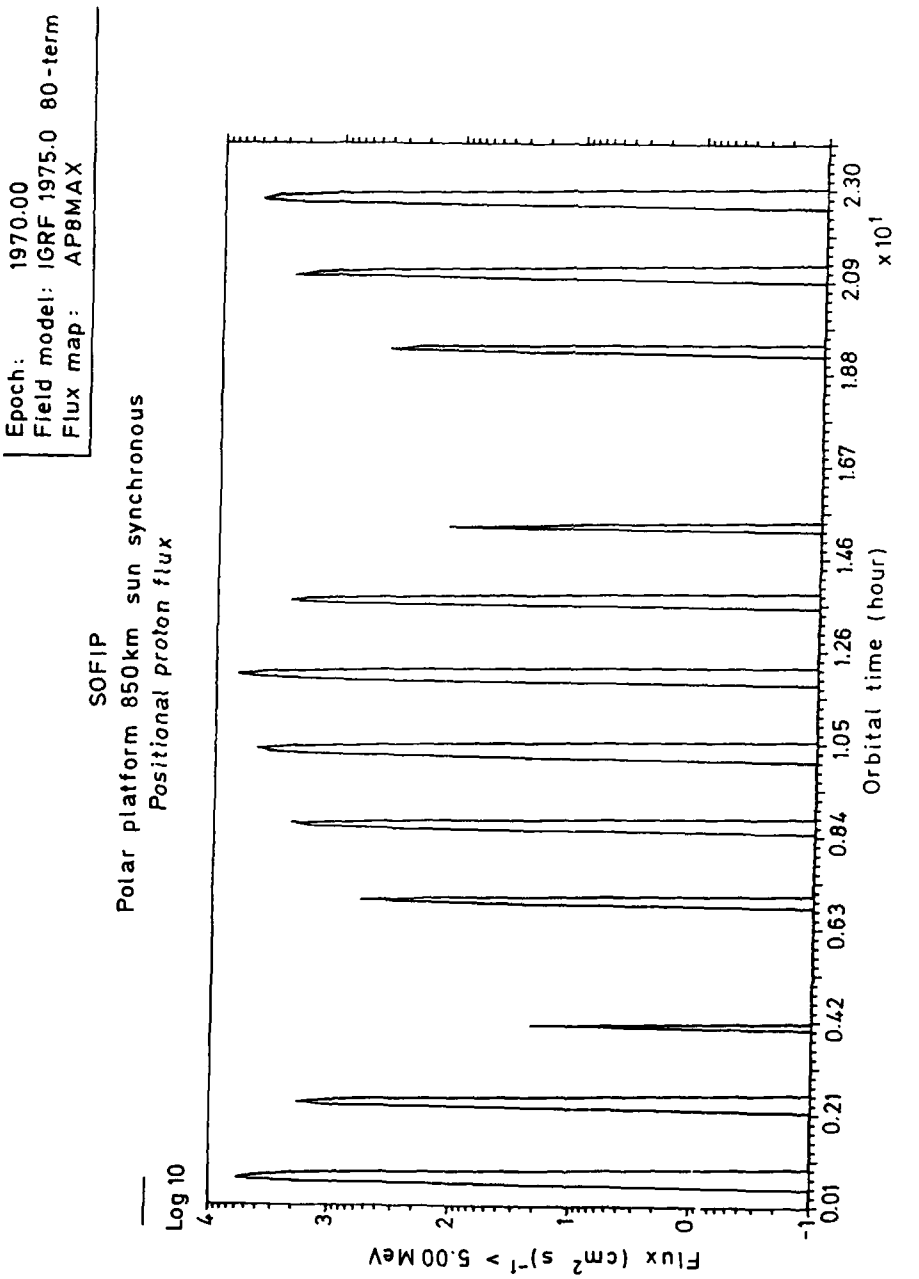

Fig 4 Positional proton flux

TR 89014

Epoch: 1970.00
Field model: IGRF 1975.0 80-term
Flux maps: AE8MAX, AP8MAX

SOFIP
Polar platform 850km sun synchronous
Integral proton and electron spectra

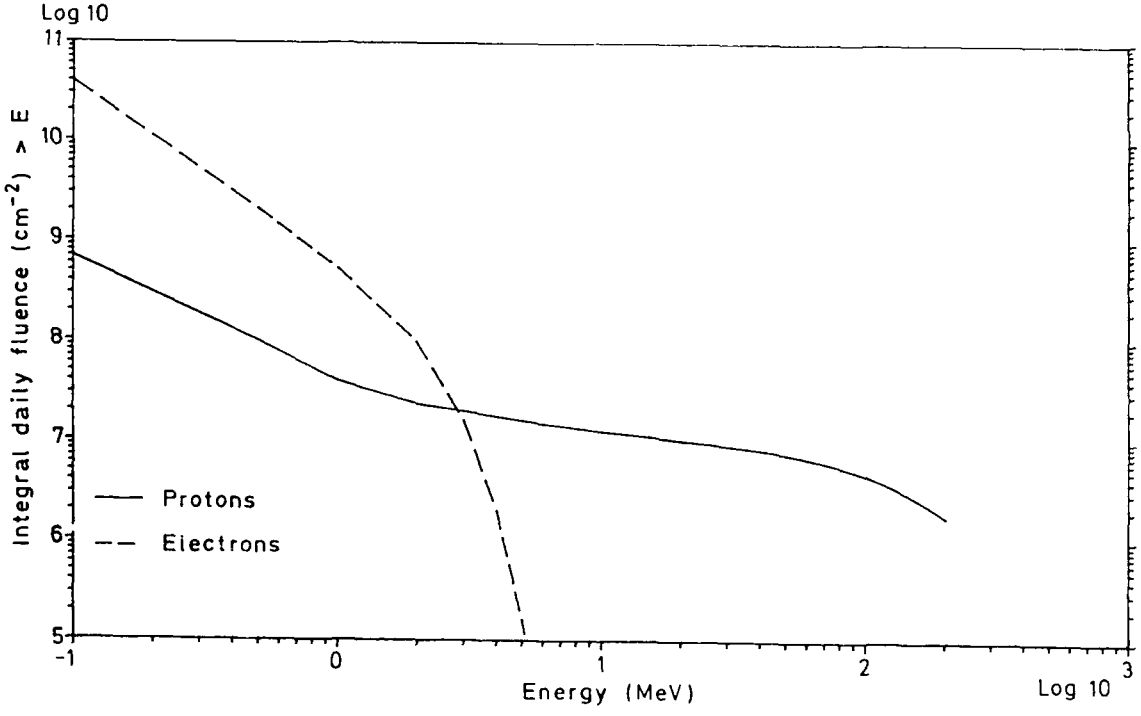

Fig 5 Integral proton and electron spectra

Fig 5

Fig 6

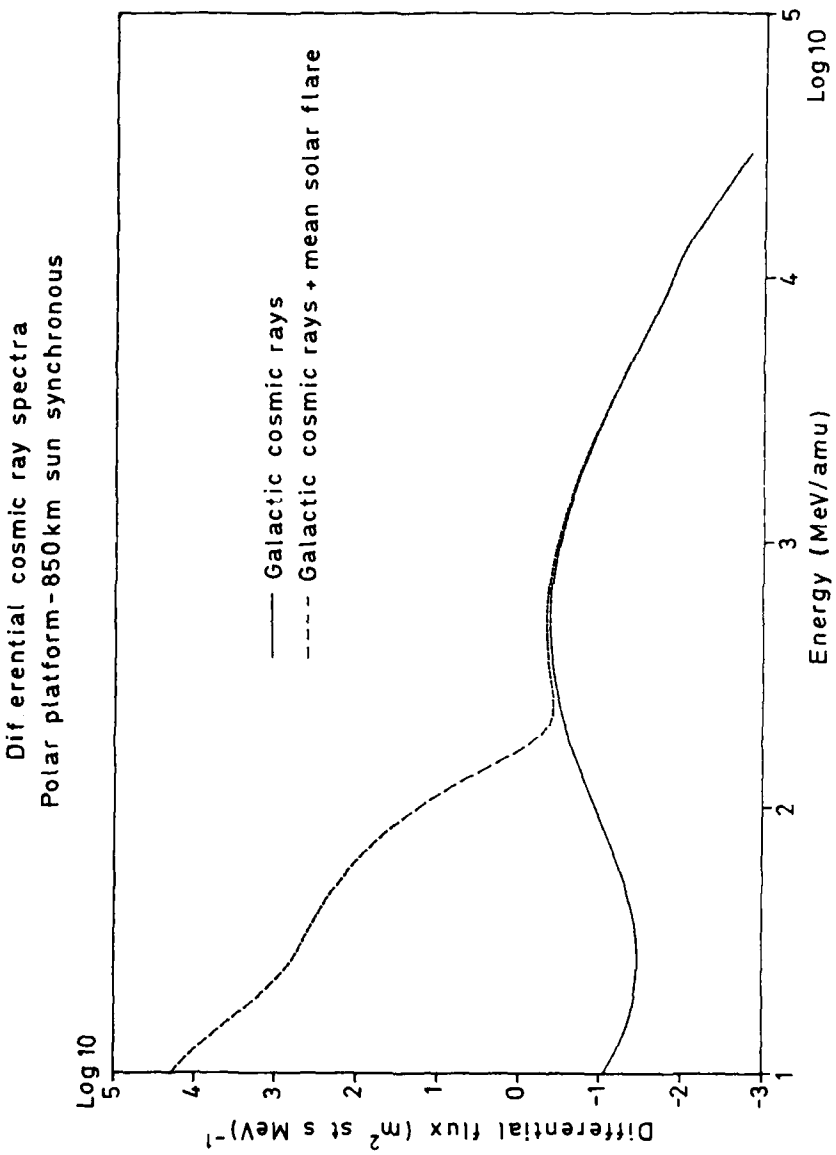

Fig 6 Differential cosmic ray spectrum

TR 89014

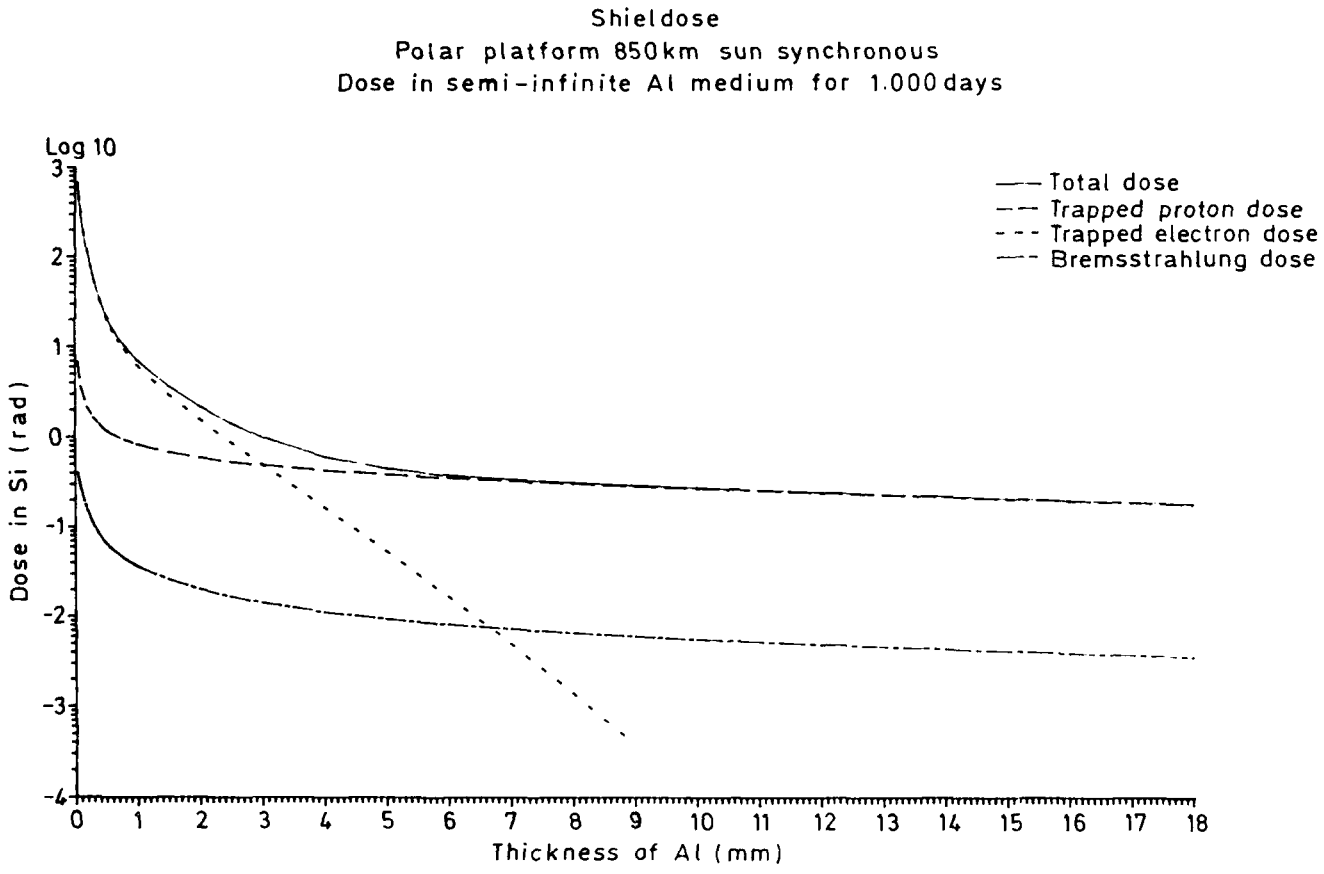

Fig 7 Dose behind a semi-infinite aluminium slab

Fig 7

Fig 8

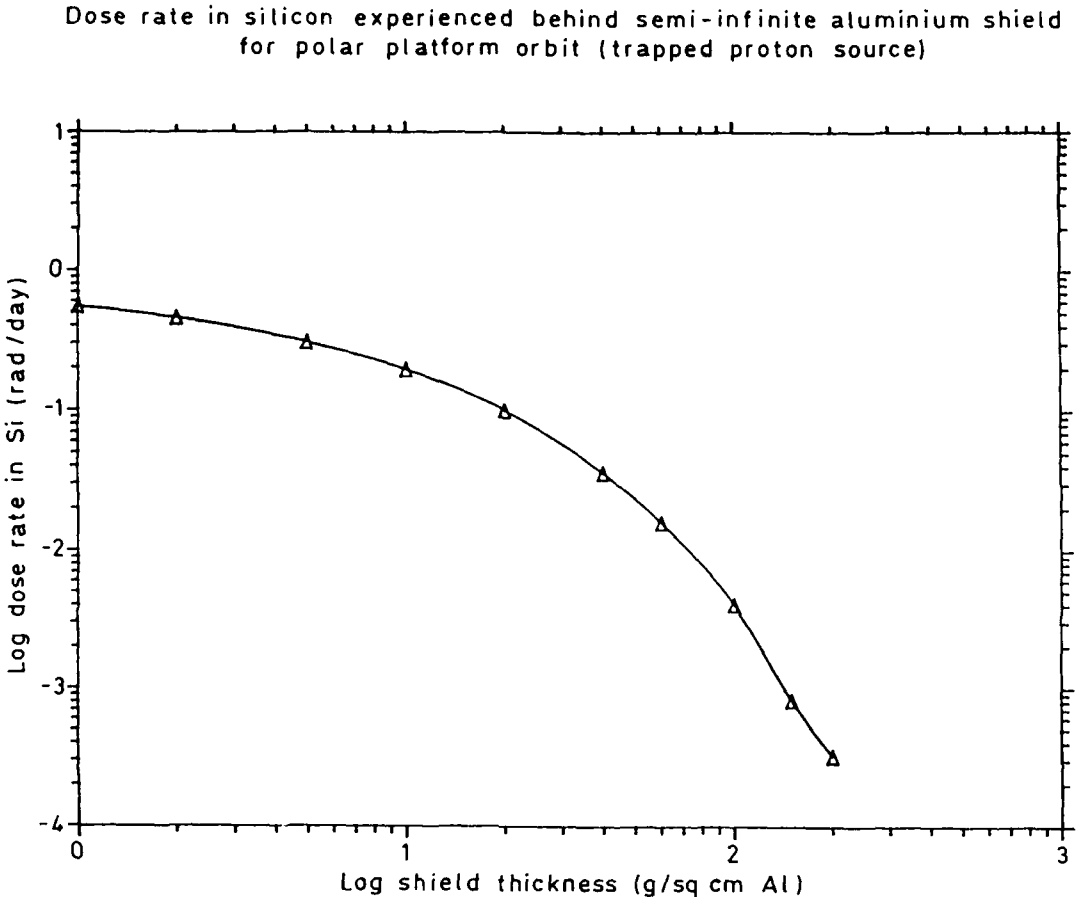

Fig 8 Dose rate behind a semi-infinite aluminium slab

TR 89014

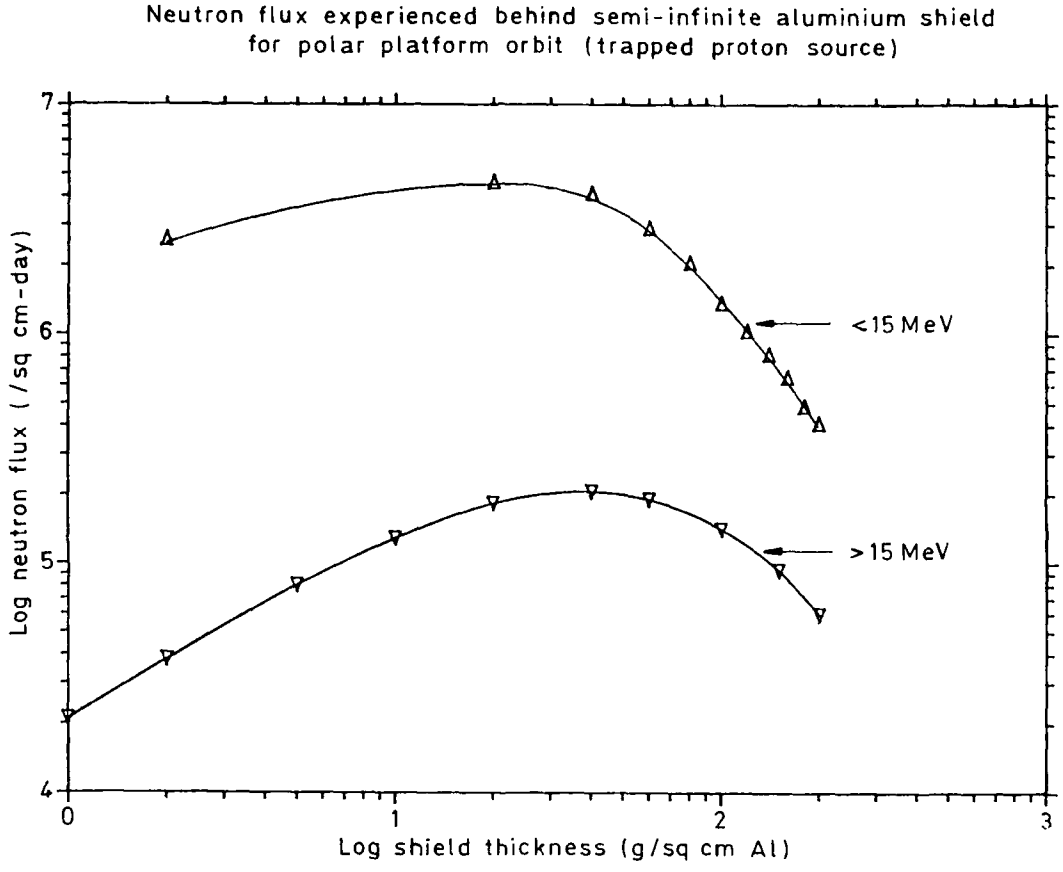

Fig 9 Neutron flux behind a semi-infinite aluminium slab

Fig 9

Fig 10

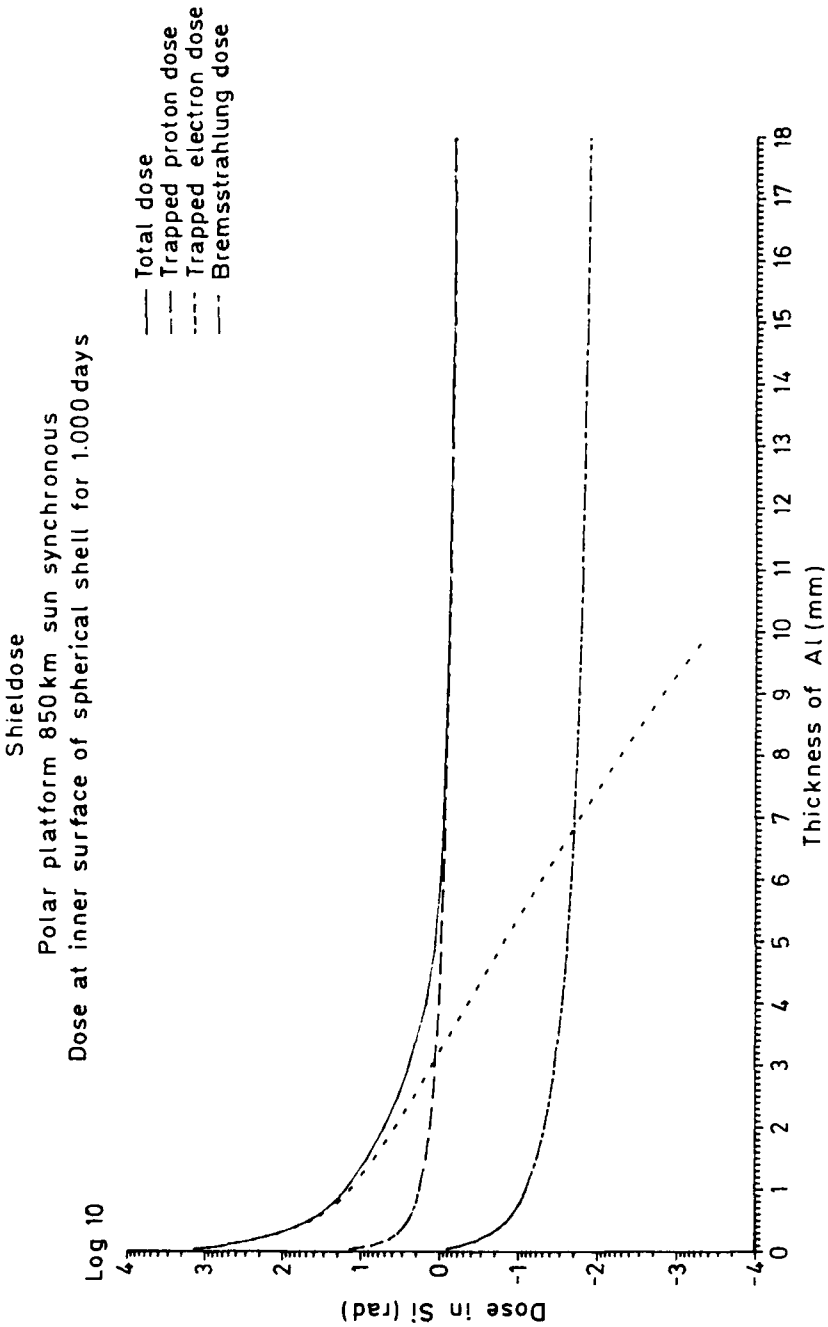

Fig 10 Dose at the inner surface of a spherical shell

TR 89014

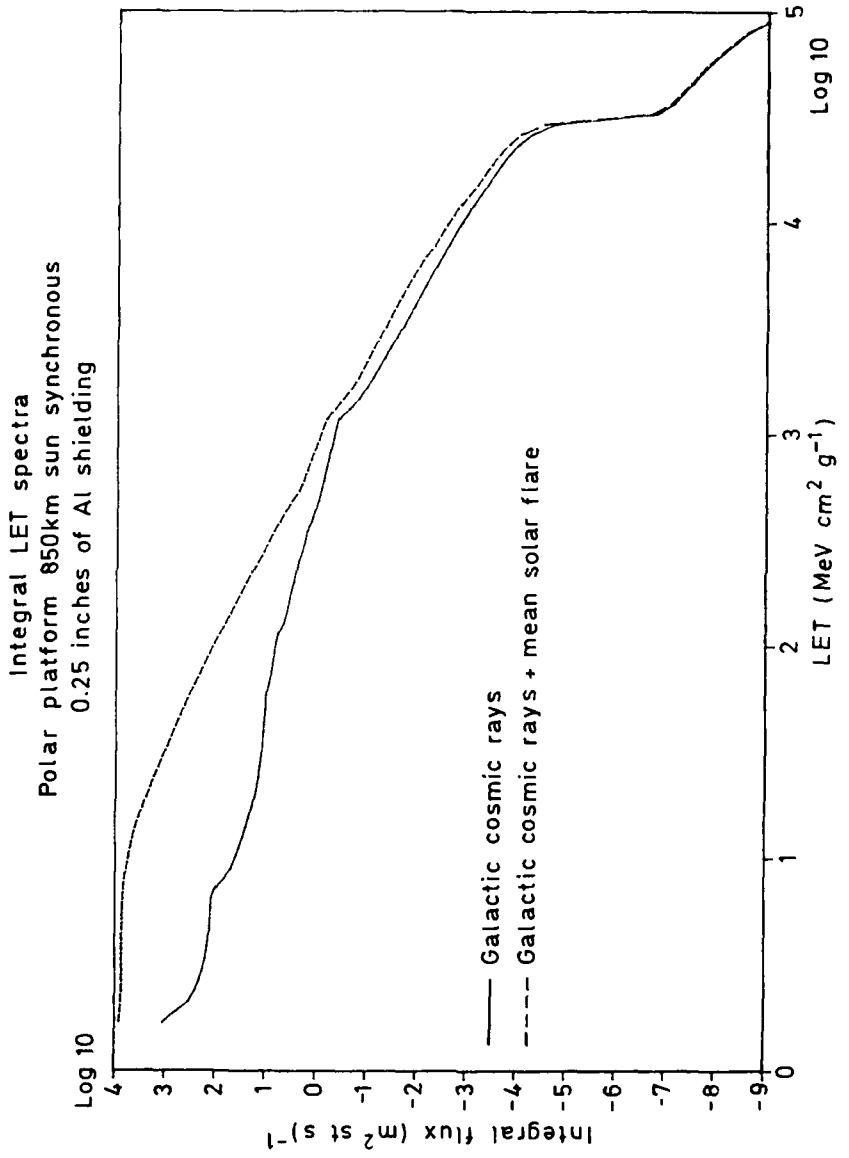

Fig 11 Integral LET spectra

REPORT DOCUMENTATION PAGE

Overall security classification of this page

UNLIMITED

As far as possible this page should contain only unclassified information. If it is necessary to enter classified information, the box above must be marked to indicate the classification, e.g. Restricted, Confidential or Secret.

1. DRIC Reference (to be added by DRIC)	2. Originator's Reference	3. Agency Reference	4. Report Security Classification/Marking
	RAE TR 89014		UNLIMITED

5. DRIC Code for Originator	6. Originator (Corporate Author) Name and Location
7673000W	Royal Aerospace Establishment, Farnborough, Hants, UK
5a. Sponsoring Agency's Code	6a. Sponsoring Agency (Contract Authority) Name and Location

7. Title

Environmental constraints for polar platform design

7a. (For Translations) Title in Foreign Language

7b. (For Conference Papers) Title, Place and Date of Conference

8. Author 1. Surname, Initials	9a. Author 2	9b. Authors 3, 4	10. Date	Pages	Refs.
Sims, A.J.	Truscott, P.R.	Wrenn, G.L. Dyer, C.S.	March 1989	26	19

11. Contract Number	12. Period	13. Project	14. Other Reference Nos.
			Space 674

15. Distribution statement

(a) Controlled by – Head of Space Department, RAE

(b) Special limitations (if any) –

If it is intended that a copy of this document shall be released overseas refer to RAE Leaflet No.3 to Supplement 6 of MOD Manual 4.

16. Descriptors (Keywords) (Descriptors marked * are selected from TEST)

17. Abstract

The considerable investment implicit in large space platforms makes assessment of both their environment and their environmental interactions of utmost importance. In this Report the new factors of relevance to the Polar Platform are reviewed, and environment models and radiation transport codes are employed to assess primary and secondary particle fluxes, dose rates and energy-loss spectra. Monitors are described which can improve the data base.

15910/1